Microelectronics Reliability 51 (2011) 2216–2222

Contents lists available at ScienceDirect

Microelectronics Reliability

journal homepage: www.elsevier.com/locate/microrel

The effects of 12 MeV electron irradiation on the electrical characteristics of the Au/Aniline blue/p-Si/Al device

Şakir Aydoğan [a,*], Ümit İncekara [b], Abdulmecit Türüt [a]

[a] Department of Physics, Faculty of Sciences, Atatürk University, 25240 Erzurum, Turkey
[b] Department of Biology, Faculty of Sciences, Atatürk University, 25240 Erzurum, Turkey

ARTICLE INFO

Article history:
Received 3 February 2011
Received in revised form 1 June 2011
Accepted 2 June 2011
Available online 20 July 2011

ABSTRACT

An Au/Aniline blue (AB)/p-Si/Al structure has been fabricated and then the effect of electron irradiation (12 MeV electron energy and 5×10^{12} e^{-} cm^{-2} fluence) on the contact parameters of the device has been analysed by using the current–voltage (I–V), capacitance–voltage (C–V), and conductance–voltage (G/w–V) measurements, at room temperature. Since the organic layer creates a physical barrier between the metal and the semiconductor, it has been seen that the AB layer causes an increase in the effective barrier height of the device. Cheung functions, Norde model and conductance method have been used in order to determine the diode parameters. The values of the ideality factor, barrier height and series resistance increased after the electron irradiation. This has been attributed to a decrease in the net ionized dopant concentration that occurred as a result of electron irradiation.

1. Introduction

Recently, extensive researches have been carried out for applying semiconducting organic materials to electronic devices such as organic light emitting diodes, Schottky diodes, organic solar cells and organic field effect transistors. Thus, semiconducting organic materials can be used in various condensed matter physics applications.

It is well known that the interfacial properties of metal/semiconductor (MS) contacts has a dominant influence on device performance, reliability and stability. In most practical MS contacts, it might be occurred a native thin insulating layer of oxide on the surface of the semiconductor This layer converts the MS structure into a metal/insulator/semiconductor device [1]. Furthermore, it can be constructed an organic thin film between metal and inorganic semiconductor intentionally. This film modifies some electrical parameters of the rectifying devices. For example, Schottky barrier heights of MS contacts can be manipulated by insertion of a dipole layer between the semiconductor and the organic film. So far many attempts have been made to realize a modification and the continuous control of the barrier height using an organic semiconducting layer, an insulating layer and/or a chemical passivation procedure at certain metal/inorganic semiconductor interfaces [2–15]. Aniline blue is a mixture of methyl blue and water blue. Molecular formula of Aniline blue (AB) is $C_{32}H_{25}N_3S_3O_9Na_2$ and it has been used an interfacial layer in our study.

The radiation effect on semiconductor-based devices is a very important subject. It is clear from that the developments in the semiconductor industry are not driven primarily with space applications or radiation hardness in mind. It is felt, therefore, that there is a need to have a clear view of potential radiation damage problems, even at an early stage of the development of the latest technology generations. This is not only important for the space community itself but can be beneficial during the process/technology development as well. The reason is that during device or circuit fabrication more and more processing steps used an aggressive environment where irreversible radiation damage can occur. So a fundamental understanding of radiation damage mechanisms and degradation is not only of use for the nuclear/space engineer, but may be helpful for the process engineer as well. It is known that there are two types of basic radiation-damage mechanisms for devices; ionisation damage and displacement lattice damage. Ionisation of the material creates free charge which can move in the material. This damage is generally harmless for the device operation. But, displacement lattice damage in semiconductor based devices can have a significant impact on their electrical properties, through the creation of stable radiation defects, which have one and/or more levels in the bandgap. Free carrier mobility and density, resistivity and generation and recombination lifetimes will be affected by displacement lattice damage. Since, all electronic devices communicate with each other over the metal/semiconductor contacts in electronic circuits, it is important to determine how the parameters of the MS contacts give a response to the electron irradiation. Although various deformations caused by the effects of the radiation have been known, there is not yet a precise explanation of deformation for all types and all parameters of crystals and devices.

* Corresponding author. Tel.: +90 442 231 4073; fax: +90 442 236 0948.
E-mail address: saydogan@atauni.edu.tr (Ş. Aydoğan).

0026-2714/$ - see front matter © 2011 Elsevier Ltd. All rights reserved.
doi:10.1016/j.microrel.2011.06.002

But in general, the exposure of these devices to high-energy particles results in a considerable amount of lattice defects. These defects act as recombination centers or minority/majority carrier trapping centers, cause degradation of the diode performance and the effects of the irradiation should be considered in device applications [15–19]. The main purpose of this study is to fabricate an Au/Aniline blue (AB)/p-Si/Al device and to investigate the effect of electron irradiation with 12 MeV electron energy and 5×10^{12} e^- cm^{-2} fluence on the electrical measurements of the device, at room temperature. Irradiations were carried out by a Siemens–Primus linear electron accelerator.

2. Experimental details

It has been used a *p*-type Si semiconductor wafer with (1 0 0) orientation and 400 μm thickness and 1–10 Ω cm resistivity. The wafer has been cleaned by the conventional Si cleaning process. The ohmic contact has been made by evaporating the Al metal on the back of the p-Si substrate, and then has been annealed at 580 °C for 3 min in N_2 atmosphere. The native oxide on the front surface of the substrate was removed in HF + 10H_2O solution. Finally, it was rinsed in deionised water (DI) for 30 s, and then has been dried. The solid AB organic layer was directly formed by adding 4 μL of Aniline blue organic material solution in alcohol (96%) on the front surface of the p-Si wafer, and evaporated by itself for drying of solvent in N_2 atmosphere for about 2 h. The thickness of the AB has been calculated from capacitance measurements as 90 nm. Then, Au metal has been evaporated on the AB layer at 10^{-5} torr (diode area = 7.85×10^{-3} cm^2). The current–voltage (*I–V*) and capacitance–voltage–frequency (*C–V–f*) and conductance/series resistance–voltage (G/R_S–*V*) measurements of the Au/AB/p-Si structure under 12 MeV-energy electron irradiation have been performed with a KEITHLEY 487 Picoammeter/Voltage Source and an HP 4192 A (5 Hz–13 MHz) LF IMPEDANCE ANALYZER, respectively, at room temperature. No bias voltage was applied to the device during the irradiation.

3. Results and discussion

The measured *I–V* characteristics of the structure have been analyzed using the conventional thermionic emission theory (TE) [1]:

$$I = I_0\left[\exp\left(\frac{qV}{nkT}\right) - 1\right], \tag{1}$$

where

$$I_o = AA^*T^2 \exp\left(-\frac{q\Phi_b}{kT}\right), \tag{2}$$

is the saturation current, Φ_b is the effective barrier height at zero bias, A^* is Richardson constant which equals to 32 Acm^{-2} K^{-2} for *p*-type Si, *q* is the electronic charge, *V* is the applied voltage, *A* is the diode area, *k* is Boltzmann constant, *T* is the absolute temperature in Kelvin, *n* the ideality factor, and it is determined from the slope of the linear region of the forward bias ln *I–V* characteristic through the relation:

$$n = \frac{q}{kT}\frac{dV}{d(\ln I)}. \tag{3}$$

n equals to unity for an ideal diode. However, *n* has usually a value greater than unity. High values of *n* can be attributed to the presence of the interfacial thin layer, a wide distribution of low-Schottky barrier height (SBH) patches (or barrier inhomogeneities) and to the bias voltage dependence of the SBH [1]. Φ_b is the zero-bias barrier height (BH), which can be obtained from the following equation:

$$\Phi_b = kT/q \ln(AA^*T^2/I_0). \tag{4}$$

Fig. 1 depicts the forward and reverse bias current–voltage (*I–V*) characteristics of the Au/AB/p-Si/Al device for unirradiated and irradiated with electron beams. The effect of electron irradiation is seen very clearly in the figure. The *I–V* plots indicate that the resistivity of the material has increased after electron irradiation and electron irradiation has caused to some reduction in forward bias currents and increment in reverse bias currents. The radiation-induced degradation observed in the reverse *I–V* characteristics might be attributed to an increase in interfacial defect density [20]. The values of the barrier heights (BHs) for before and after electron irradiation have been calculated as 0.75 and 0.77 eV, respectively. In addition, the values of the ideality factors for before and after irradiation have been calculated as 2.17 and 2.26, respectively. The high values in the ideality factor are possibly caused by an organic interlayer plus a native oxide film between the top metal and the inorganic semiconductor. Although the native oxide layer has been removed by the cleaning procedure, it is inevitable to form a thin oxide layer during to vacuum process and before deposition of the organic layer too. This oxide layer has a insulating layer for Si and it causes non-ideal *I–V* characteristics. The interfacial parameters such as the interface states and interfacial layer cause strong masking of the electrical characteristics of the Schottky barrier diodes. Furthermore, the high value of the ideality factor indicates that current transport mechanism is not thermionic emission. According to the experimental results, barrier height and the ideality factor values increased by electron irradiation. This may be due to the introduction of irradiation induced defects at the interface between the AB layer and p-Si substrate. The irradiation of materials by high-energy particles is known to introduce lattice defects and the semiconductor properties are sensitive to defect concentrations [1,20–22]. Namely, the

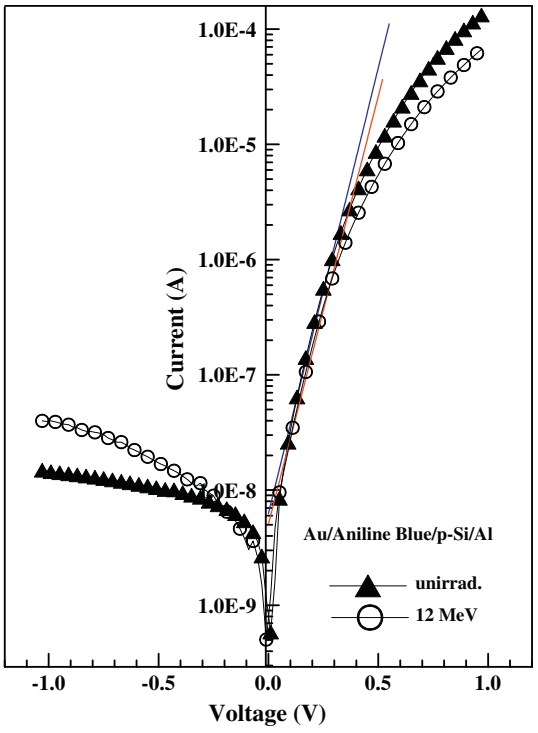

Fig. 1. The forward and reverse bias current–voltage (*I–V*) characteristics of the Au/AB/p-Si/Al for unirradiated and irradiated with 12 MeV electron energy.

increase in the reverse current and in the barrier height of the potential barrier are due to the irradiation induced defects at the interface. As more defects are introduced by electron irradiation, the effective carrier lifetime decreases and the recombination current increases. Also, the recombination current is dominant in forward bias condition, and then the diode ideality factor increases.

For metal/semiconductor contacts, the series resistance is an important parameter, affecting the electrical characteristics of Schottky diodes. The Schottky diode parameters such as the barrier height, the ideality factor, and the series resistance can also be achieved using a method developed by Cheung and Cheung [23].

According to [23], the forward bias *I–V* characteristics due to the TE of a Schottky diode with the series resistance can be expressed as:

$$I = I_0 \exp\left[\frac{q(V - IR_s)}{nkT}\right], \tag{5}$$

where the IR_s term is the voltage drop across series resistance of device. The values of the series resistance can be determined from the following functions using Eq. (5):

$$\frac{dV}{d(\ln I)} = \frac{nkT}{q} + IR_s, \tag{6}$$

$$H(I) = V - \left(\frac{nkT}{q}\right)\ln\left(\frac{I}{AA^*T^2}\right), \tag{7}$$

and $H(I)$ is given as follows:

$$H(I) = n\Phi_b + IR_s. \tag{8}$$

A plot of $\frac{dV}{d(\ln I)}$ *vs. I* will be linear and gives R_s as the slope and $\frac{nkT}{q}$ as the *y*-axis intercept from Eq. (6). Figs. 2 and 3 show the plots of $\frac{dV}{d(\ln I)}$ and $H(I)$ *vs. I* for Au/AB/p-Si/Al structure. From Eq. (6) the values of n and R_s have been calculated as $n = 3.43$, $R_s = 1663\ \Omega$ and $n = 3.77$, $R_s = 3152\ \Omega$, for before and after irradiation (12 MeV) cases of the structure, respectively. Using the value of the n obtained from Eq. (5), the value of Φ_b is obtained from plot of a function $H(I)$ given by (8). From $H(I)$ *vs. I* plots, the values of the Φ_b and R_S have been calculated as $\Phi_b = 0.76$ eV, $R_s = 1739\ \Omega$ and $\Phi_b = 0.79$ eV, $R_s = 3214\ \Omega$, for the pre-irradiation and 12 MeV electron irradiation, respectively. It can be obviously seen that the values of R_s obtained from $H(I)$–*I* curve are in close agreement with

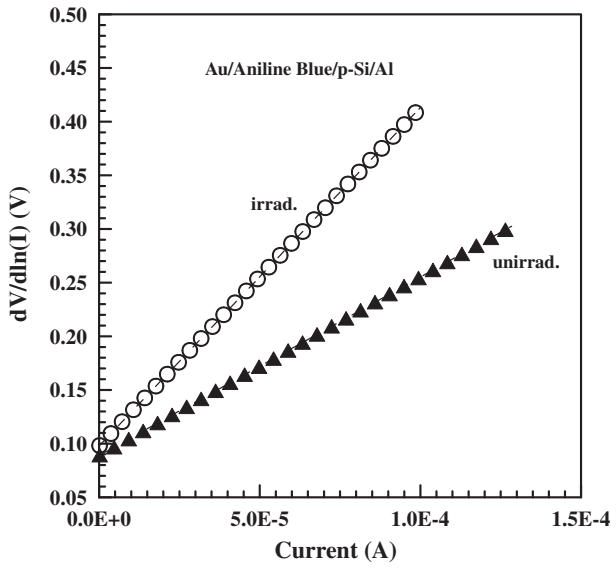

Fig. 2. A plot of $\frac{dV}{d(\ln I)}$ *vs. I* for Au/AB/p-Si/Al structure for before and after electron irradiation.

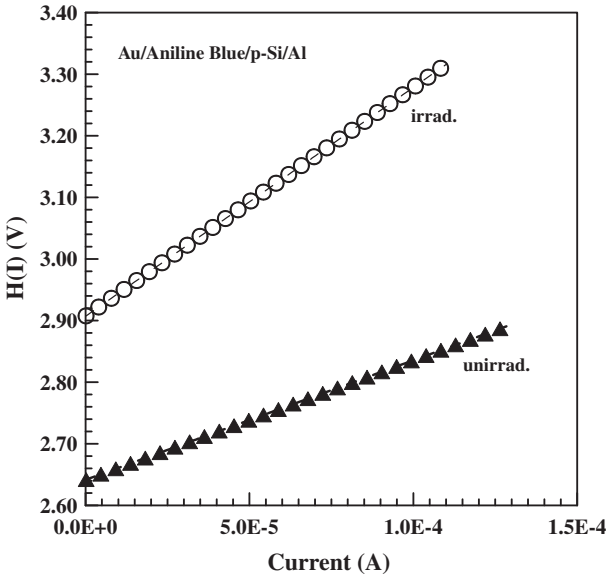

Fig. 3. A plot of $H(I)$ *vs. I* for Au/AB/p-Si/Al structure for before and after electron irradiation.

the values obtained from the $dV/d(\ln I)$–*I* plot. However, there is a seriously increase in the series resistance value after 12 MeV electron irradiation. The modification of Schottky barrier characteristics due to interaction with electron beam can be understood by considering the basic phenomena of energy loss of the electron as it passes through the metal–semiconductor interface. As is well known, the nuclear energy loss mainly causes displacement of target atoms leading to defects like vacancies and interstitials, and this can increase the density of states at metal/semiconductor (MS) interface. The electronic energy loss causes excitations of target electrons, and during the relaxation of these electrons various defects like vacancies, interstitials, mixing at the MS interface, and other complex defects are created. These defects have their energy levels lying deep inside the band gap of the semiconductor, which leads to the introduction of interface states at MS interface, which modifies the current transport properties across the Schottky barrier [24–26].

In the determination of the series resistance an alternative method was proposed by Norde [27] as follows:

$$F(V) = \frac{V}{\gamma} - \frac{kT}{q}\ln\left(\frac{I(V)}{AA^*T^2}\right), \tag{9}$$

where γ is an integer (dimensionless) greater than ideality factor. $I(V)$ is current obtained from the *I–V* curve. Once the minimum of the *F vs. V* plot is determined, the value of barrier height can be obtained from Eq. (10), where $F(V)$ is the minimum point of $F(V)$ and V_0 is the corresponding voltage.

$$\Phi_b = F(V) + \frac{V_0}{\gamma} - \frac{kT}{q}. \tag{10}$$

Fig. 4 depicts the $F(V)$–*V* plot of the structure. From Norde's functions, R_s value can be determined from the following equation:

$$R_s = \frac{kT(\gamma - n)}{qI} \tag{11}$$

From the *F–V* plots, the values of Φ_b and R_s of the structure have been calculated as 0.79 eV and 3303 Ω for the unirradiated and 0.81 eV and 3508 Ω for after 12 MeV electron irradiation, respectively. It has been seen that the values of the series resistance and barrier height obtained from both Cheung and Norde methods

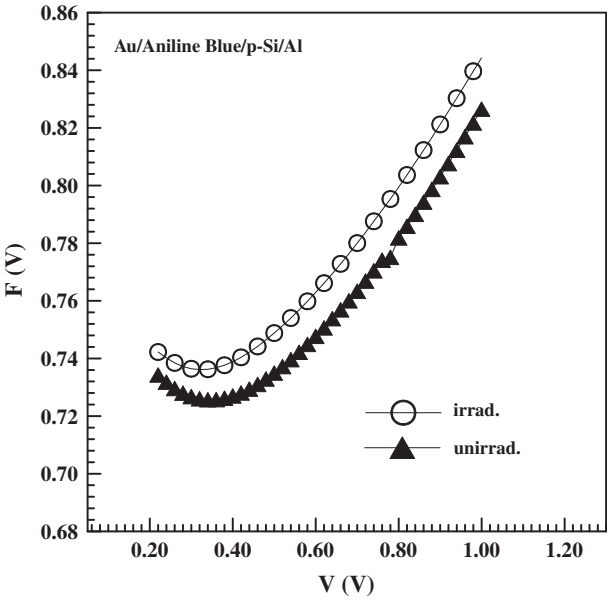

Fig. 4. *F*(*V*) *vs. V* plots of the Au/AB/p-Si/Al structure for unirradiated and irradiated case.

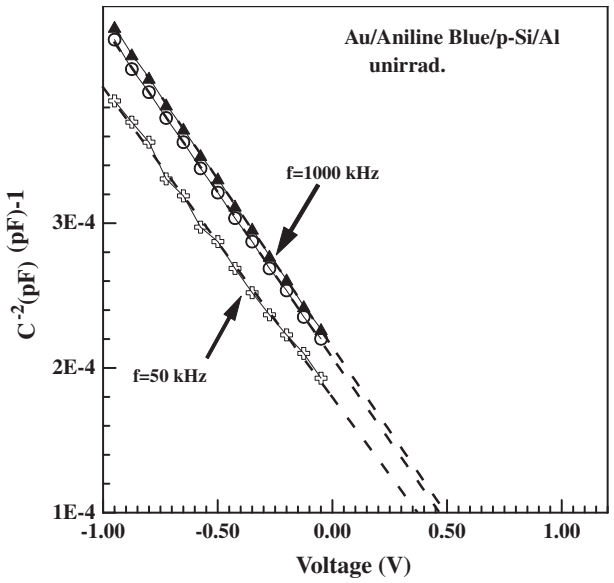

Fig. 6. The reverse bias C^{-2}–V characteristics of the Au/AB/p-Si/Al structure before electron irradiation at various frequencies.

increased after electron irradiation. An increase in series resistance indicates that the product of the mobility and the free carrier concentration has reduced. The reduction in mobility is due to the introduction of defect centers with irradiation which act as scattering centers. The free carrier concentration will be reduced if deep traps are introduced into the material associated with point defect displacement damage. Free carriers in the crystal lattice are captured by these defect centers resulting in decreased carrier density. The density of radiation-induced defect centers increases with increasing irradiation leading to increased carrier removal [16,28].

Figs. 5 and 7 show the forward and the reverse bias C–V plots and Figs. 6 and 8 show the reverse bias $1/C^2$–V plots of the device measured at various frequencies for unirradiated and irradiated by electron beam, respectively. It can be seen that in reverse bias, the

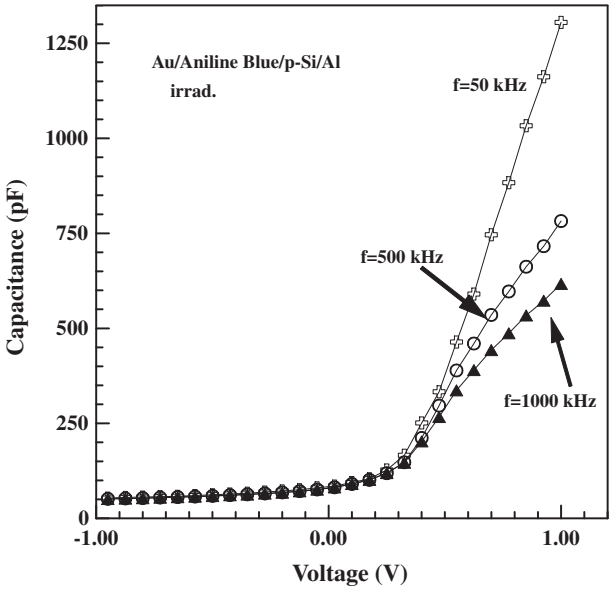

Fig. 7. The forward and reverse bias C–V characteristics of the Au/AB/p-Si/Al structure after electron irradiation at various frequencies.

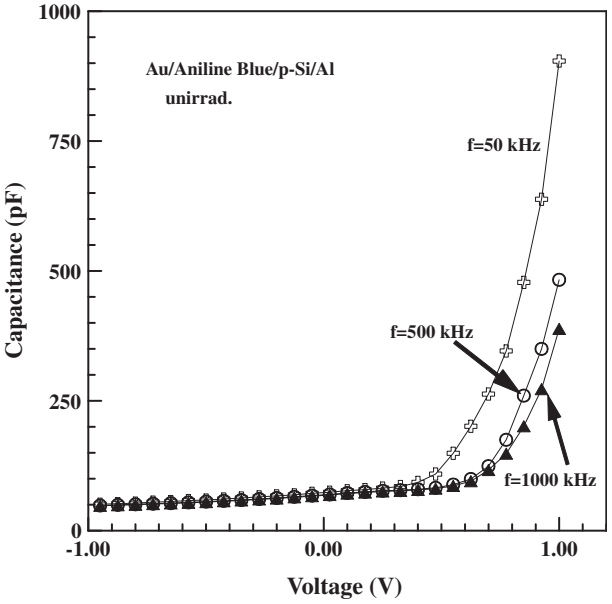

Fig. 5. The forward and reverse bias C–V characteristics of the Au/AB/p-Si/Al structure before electron irradiation at various frequencies.

value of the capacitance is monotonically increasing towards the low negative voltages and it is sharply increasing in forward bias towards the high voltages. The higher values of the capacitance at low frequencies are due to the excess capacitance resulting from the interface states in equilibrium with the *p*-Si that can follow the alternating current (a.c.) signal. Namely, the interface states at lower frequencies follow the a.c. signal, whereas at higher frequencies they cannot follow the alternating current signal. At the high frequencies, the values of the capacitance are only space charge capacitance. From the capacitance–voltage measurements the values of the barrier heights have been calculated as 0.82 and 0.87 at f = 500 kHz for before and after electron irradiation, respectively. The C–V curves gave a Schottky barrier height (BH) value higher than those derived from the I–V measurements. This discrepancy can be explained by the different nature of the C–V and I–V mea-

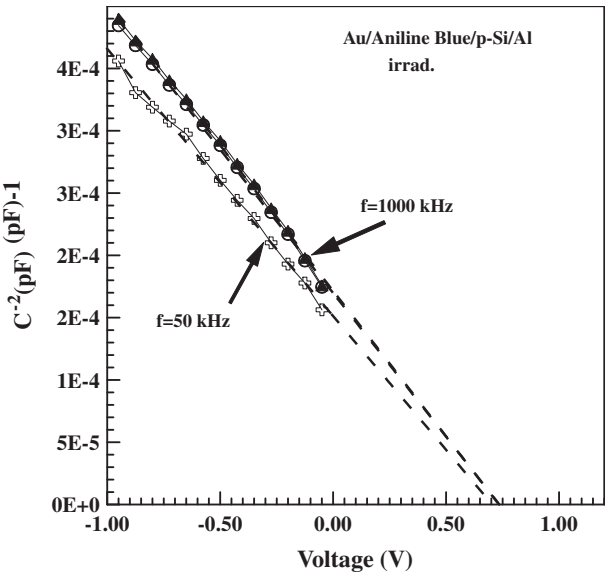

Fig. 8. The reverse bias C^{-2}–V characteristics of the Au/AB/p-Si/Al structure after electron irradiation.

surement techniques. In general, the barrier heights deduced from two techniques are not always the same. If the barriers are uniform and ideal, the two measurements yield the same value; otherwise, they will yield different values. The different behavior of BHs obtained from the two techniques can be explained by a distribution of BHs due to the inhomogeneties (as a combination of the interfacial oxide layer composition, non-uniformity of the interfacial AB layer thickness, and distribution of interfacial charges) that occur at metal/semiconductor interface [9,29]. Besides, the increase in barrier height, obtained from the C–V characteristics, is due to an increase in diffusion potential as shown in Figs. 6 and 8. The diffusion potential at zero bias which is determined from an extrapolation of the linear C^{-2}–V plot to the V-axis. The slightly variation of capacitance at 12 MeV electron energy might be due to the creation of radiation-induced a small number of defects at the interface of the structure through the change in carrier concentration, minority carrier life time and carrier mobility. The high values of the capacitance may be attributed to increase in the net ionized dopant concentration with electron irradiation. However, this poor variation of the capacitance might be attributed to the slight electron irradiation effects on the concentration of deep level defects.

In some contacts the capacitance under forward bias is larger than the space-charge capacitance predicted by basic theory. The difference between the measured and the space-charge capacitance is called the excess capacitance and is attributed to interface states. The interface states can be created by crystal lattice discontinuities (dangling bonds), interdiffusion of atoms or a large density of crystal lattice defects close to the metal/semiconductor interface or organic/semiconductor interface. The interface states capacitance is a function of the forward bias current and frequency. The magnitude of the capacitance related to the interface states is relatively small. For low forward currents, the capacitance can be measured using standard impedance and capacitance meters. For large forward currents, the signal related to the interface states capacitance is overwhelmed by the thermionic emission conductance and more sophisticated, high accuracy measurement techniques are required. Schottky capacitance spectroscopy (SCS) is a measurement technique which can provide the required accuracy in the interface states capacitance measurements. The technique is based one strong dependence of the semiconductor junction differential admittance on the temperature and measurement ac signal frequency in the case of a semiconductor with an incompletely ionized impurity. In general, the C–f plots in the idealized case are frequency independent. However, this idealized case is often disturbed due to the presence of the interface states at the interfacial layer and semiconductor interface. If charge is exchanged between the interface states and the semiconductor when a small ac signal is applied, the measured junction capacitance is the sum of the space-charge and interface states capacitance [30–37].

The capacitance of MS devices depending on frequency is given as follows [37]:

$$C = C_{sc} + C_{ss} \quad \text{(at low frequency)}, \tag{12}$$

$$C \cong C_{sc} \quad \text{(at high frequency)}, \tag{13}$$

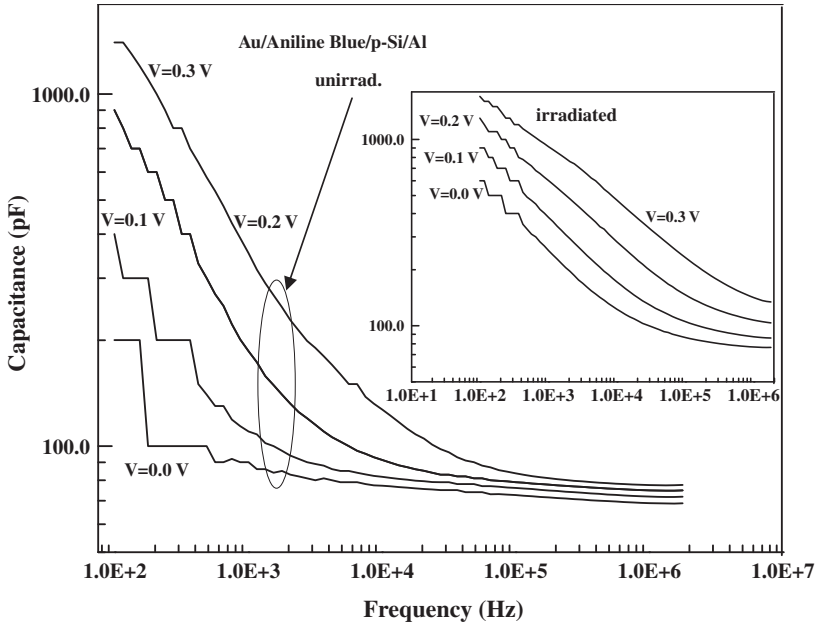

Fig. 9. The forward bias C–f characteristics of the Au/AB/p-Si/Al structure before and after (inset) electron irradiation at various voltages.

where C_{sc}; is space charge capacitance, and C_{ss}; is interface capacitance. The interface capacitance can be described as

$$C_{ss} = AqN_{ss}\frac{Arc\tan(wt)}{w\tau}, \tag{14}$$

where τ is the time constant and can be written as

$$\tau = \frac{1}{v_{th}\sigma N_d}\exp\left(\frac{qV_d}{kT}\right), \tag{15}$$

where σ is the cross section of interface states, v_{th} is the thermal velocity of the carrier, N_d is doping concentration, q is electron charge and k is Boltzmann constant. Fig. 9 shows the capacitance–frequency (C–f) characteristics for unirradiated and irradiated conditions of the structure at various biases. The values of the capacitance did not show a significant difference after electron irradiation as C–V plots but it was seen a small reduction. This can be attributed to the change in dielectric constant at the interface or to increase in the net ionized dopant concentration with electron irradiation or to electron–hole pair generation by the electron irradiation.

Conductance technique is based on the conductance losses resulting from the exchange of majority carriers between the interface states and majority carrier band of the semiconductor when a small ac signal is applied to the semiconductor devices [38]. The conductance–voltage (G/ω–V) characteristics of Au/AB/p-Si structure at the various frequencies for unirradiated and after 12 MeV electron energy are shown in Figs. 10 and 11, respectively. Where G is the measured conductance and ω the angular frequency ($\omega = 2\pi f$) of the applied electric field. It is seen that both plots are dependent on the voltage, frequency and irradiation effects. A slight increase for conductance may be attributed to the increase in the net ionized dopant concentration or the irradiation-induced excess carriers generated in the p-type Si.

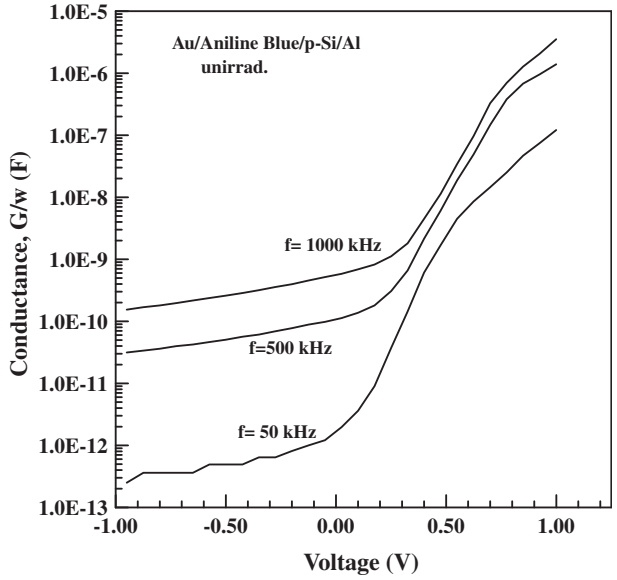

Fig. 10. The conductance–voltage plots of the Au/AB/p-Si/Al structure at various frequencies before electron irradiation.

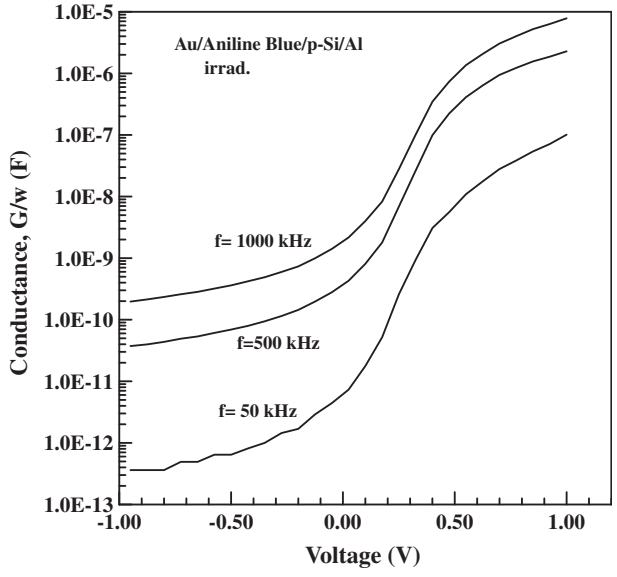

Fig. 11. The conductance–voltage plots of the Au/AB/p-Si/Al structure at various frequencies after electron irradiation.

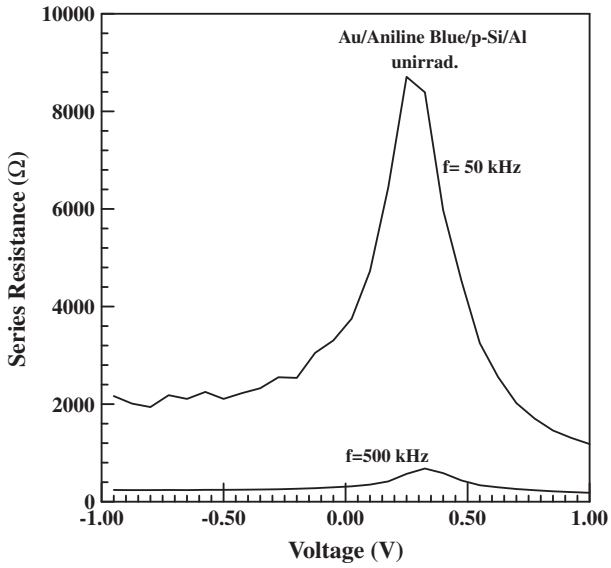

Fig. 12. The series resistance–voltage plots of the Au/AB/p-Si/Al structure before electron irradiation.

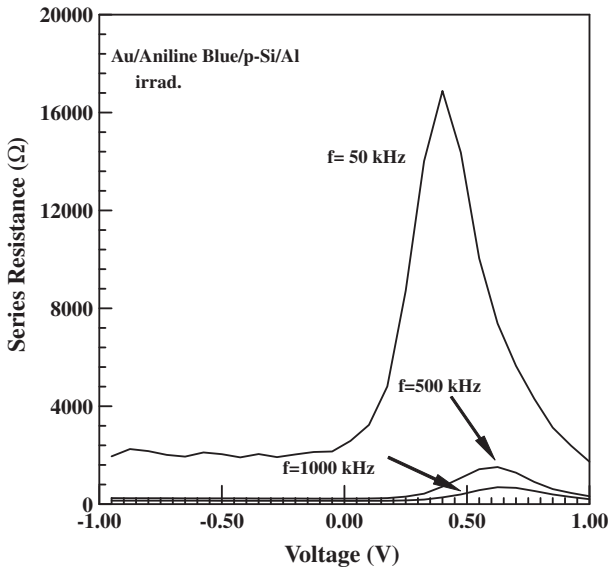

Fig. 13. The series resistance–voltage plots of the Au/AB/p-Si/Al structure after electron irradiation.

The series resistance of metal–semiconductor devices can be subtracted from the measured capacitance and conductance measurements in the strong accumulation region at high frequency. The frequency dependency of the series resistance can be obtained from the measurements of C–V–f and G/w–V–f curves as [38]

$$R_s = \frac{G_{ma}}{G_{ma}^2 + (wC_{ma})^2}, \tag{16}$$

where G_{ma} and C_{ma} are values of the conductance and capacitance obtained in the strong accumulation region at high frequency. Figs. 12 and 13 depict the series resistance–voltage (R_s–V) characteristics of the structure for unirradiated and irradiated conditions at various frequencies. The series resistance depends on both frequency and voltage and the plot gives a peak at a particular voltage which decreases with the increase in frequency. The voltage and frequency dependence of series resistance can be attributed to the particular distribution density of interface states and interfacial layer [1,39]. As shown in Figs. 12 and 13, the series resistance increased after 12 MeV electron energy. This variation of the series resistance may be attributed to particular distribution of interface states due to the irradiation induced defect states interface.

4. Conclusions

In summary, an Au/AB/p-Si/Al structure has been fabricated and the effect of 12 MeV electron irradiation on the electrical characteristics of the structure has been investigated. It is found that the electrical characteristics of the Au/AB/p-Si/Al device are very sensitive to electron irradiation. Namely, the study is focused on the effect of electron irradiation on the Au/AB/p-Si/Al device not only the AB organic layer. It has been seen that after electron irradiation the values of the barrier height, series resistance and ideality factor have been increased. Furthermore, it has been seen that the capacitance values increased slightly after electron irradiation. The degradation of the diode parameters at 12 MeV electron energy might be due to the creation of radiation-induced defects at the interface of the structure through the change in carrier concentration, minority carrier life time and carrier mobility.

References

[1] Rhoderick EH, Williams RH. Metal–semiconductor contacts. second ed. Oxford: Clarendon; 1988.
[2] Campbell IH, Rubin S, Zawodzinski TA, Kress JD, Martin RL, Smith DL, et al. Phys Rev B 1996;54(20):14321.
[3] Migahed MD, Fahmy T, Ishra M, Barakat A. Polym Test 2004;23:361.
[4] Yamamoto T, Wakayama H, Fukuda T, Kanbara T. J Phys Chem 1992;96:8677.
[5] El-Sayed SM, Hamid HMA, Radwan RM. Radiat Phys Chem 2004;69(4):339.
[6] Kang MG, Park HH. Vacuum 2002;67(1):91.
[7] Nguyen VC, Kamloth KP. J Phys D Appl Phys 2000;33:2230.
[8] El-Nahass MM, Abd-El-Rahman KF, Farag AAM, Darwish AAA. Org Electron 2005;6:129.
[9] Aydogan S, Saglam M, Turut A. Vacuum 2005;77:269.
[10] Aydogan S, Saglam M, Turut A. Polymer 2005;46:563.
[11] Vermeir IE, Kim NY, Laibinis PE. Appl Phys Lett 1999;74:3860.
[12] Musa I, Eccleston W. Thin Solid Films 1999;343–344:469.
[13] Cakar M, Yildirim N, Karatas S, Temirci C, Turut A. J Appl Phys 2006;100:074505.
[14] Roberts ARV, Evans DA. Appl Phys Lett 2005;86:072105.
[15] Karatas S, Turut A. Vacuum 2004;74(1):45.
[16] Uğurel E, Aydoğan Ş, Şerifoğlu K, Türüt A. Microelectron Eng 2008;85:2299–303.
[17] Aboelfotoh. Phys Rev B 1989;39:5070–8.
[18] Gökçen, Tataroğlu A, Altındal Ş, Bülbül MM. Radiat Phys Chem 2008;77:74–8.
[19] Claeys C, Simoen E. Radiation effects in advanced semiconductor materials and devices. Berlin, Heidelberg: Springer-Verlag; 2002 [Printed in Germany].
[20] Umana-Membreno GA, Dell JM, Parish G, Nener BD, Faraone L, Mishra UK. IEEE Trans Electron Dev 2003;50:12.
[21] Güllü Ö, Aydoğan Ş, Şerifoğlu K, Türüt A. Nucl Instrum Methods Phys Res Sect A 2008;593:544–9.
[22] Goodman SA, Auret FD, du Plessis M, Meyer WE. Semicond Sci Technol 1999;14:323.
[23] Cheung SK, Cheung NW. Appl Phys Lett 1986;49:85.
[24] Stampfli P. Nucl Instrum Meth B 1998;107:138.
[25] Singh JP, Singh R, Kanjilal D, Mishra NC, Ganesan V. J Appl Phys 2000;87:2742.
[26] Sharma AT, Shahnawaz, Kumar Sandeep, Katharria YS, Kanjilal D. Nucl Instrum Meth Phys Res B 2007;263:424–8.
[27] Norde H. J Appl Phys 1979;50:5052.
[28] Pattabi M, Krishnan S, Ganesh, Mathew X. Sol Energy 2007;81:111.
[29] Coskun C, Aydogan S, Efeoglu H. Semicond Sci Technol 2004;19(2):242–6.
[30] Deneuville AJ. J Appl Phys 1974;45:3079.
[31] Barret C, Vapaille A. Solid-State Electron 1975;18:25.
[32] Zamora M, Gazecki J, Reeves GK. Solid-State Electron 1995;38(10):1771.
[33] Chattopadhyay P, RayChaudhuri B. Solid-State Electron 1993;36:605.
[34] Werner JH, Ploog K, Queisser HJ. Phys Rev Lett 1986;57:1080.
[35] Akal B, Benamara Z, Gruzza B, Bideux L. Vacuum 2000;57:219.
[36] Aydogan Ş, Saglam M, Turut A. Polymer 2005;16:6148–53.
[37] Nicollian EH, Goetzberger A. Bell Syst Tech J 1967;46:1055–133.
[38] Nicollian EH, Goetzberger A. Appl Phys Lett 1965;7(8):216–9.
[39] Karataş Ş, Türüt A, Altındal Ş. Radiat Phys Chem 2009;78:130–4.